

Local Discontinuity Measures for 3-D Seismic Data

Israel Cohen*

*Department of Electrical Engineering
Technion - Israel Institute of Technology
Technion City, Haifa 32000, Israel*

Ronald R. Coifman†

*Department of Mathematics
Yale University
New Haven, CT 06520, USA*

Abstract

In this work, an analysis method is developed for the robust and efficient estimation of 3-D seismic local structural entropy, which is a measure of local discontinuity. This method avoids the computation of large covariance matrices and eigenvalues, associated with the eigenstructure-based and semblance-based coherency estimates. We introduce a number of local discontinuity measures, based on the relations between subvolumes (quadrants) of the analysis cube. The scale of the analysis is determined by the type of geological feature that is of interest to the interpreter. By combining local structural entropy volumes using various scales, we obtain a higher lateral resolution and better discrimination between incoherent and coherent seismic events. Furthermore, the method developed is computationally much more efficient than the eigenstructure-based coherency method. Its robustness is demonstrated by synthetic and real data examples.

*E-mail: icohen@ee.technion.ac.il; Tel.: +972 4 8294731; Fax: +972 4 8323041

†E-mail: coifman@math.yale.edu; Tel.: (203) 248-8212; Fax: (203) 432-0593

Introduction

One of the most challenging tasks facing the seismic interpreter is locating subtle geological features, such as faults, within a potentially enormous data volume. These geological features are significant since they are often associated with the formation of subsurface traps in which petroleum might accumulate. A major step forward in the interpretation of 3-D seismic data was the introduction of the coherency cube by Bahorich and Farmer (1995). This fundamental tool, which replaces the original seismic volume by a volume of coherency estimates, ideally gives an interpreter a much clearer visual indication of the continuity between neighboring windowed seismic traces. Unfortunately, their coherency measure is based on a classical normalized cross correlation of only three traces. This approach is computationally very efficient, but lacks robustness when dealing with noisy data (Marfurt *et al.* 1998).

Marfurt *et al.* (1998) proposed a multitrace semblance measure, which estimates coherency over an arbitrary number of traces. This measure provides a greater stability in the presence of noise, and improved vertical resolution compared to the cross correlation algorithm. However, increasing the number of traces used for the coherency analysis, decreases lateral resolution, and increases the computational cost.

Gersztenkorn and Marfurt (1999) introduced a coherence estimate based on an eigenstructure approach. Accordingly, an analysis cube enclosing a relatively small subvolume of traces is used for constructing a covariance matrix. The (i, j) th component of the covariance matrix represents the cross covariance of the i th and j th traces within the analysis cube. A coherence measure is then estimated by the ratio of the dominant eigenvalue and the trace of that covariance matrix. It was shown that the eigenstructure-based coherence estimate provides a more robust measure of coherence, when compared to the cross correlation and semblance based computations (Gersztenkorn and Marfurt 1999; Marfurt *et al.* 1999). Yet, its main drawback is the expensive calculations required

for the building of large covariance matrices and the computation of their dominant eigenvalues.

In this paper, we propose an analysis method for the estimation of seismic local structural entropy which is both robust to noise and computationally efficient. Similarly to the eigenstructure-based coherence algorithm, an analysis cube is selected by the interpreter, according to the type of geological feature that is of interest. Structural features, such as faults, having a longer vertical duration are analyzed with larger analysis cubes. Stratigraphic features, such as channels, characterized by shorter vertical duration are analyzed with smaller analysis cubes. However, the present method avoids the computation of large covariance matrices and their dominant eigenvalues. We define a small (4 by 4) correlation matrix, formed from the cross correlations of four subvolumes (quadrants) of the analysis cube. Then, the normalized trace of this matrix is used as a local structural entropy estimate. A number of alternative local discontinuity functionals are also introduced, derived from similar relations between the quadrants of the analysis cube. Synthetic and real data examples demonstrate the robustness of the proposed method. Furthermore, by combining local structural entropy volumes using various sizes of analysis cubes, higher resolutions are obtained. Specifically, the detection of features is restricted to larger-scale discontinuities, while suppressing small-scale discontinuities, which are generally not of interest to an interpreter.

Based on this work we have derived efficient methods for background rejection and detection and classification of anomalies in images and multi-dimensional data. Some methods have been successfully tested in a variety of applications including medical diagnostics, underwater mine detection and adaptive noise removal. These ideas and examples will be detailed in subsequent publications.

Local Seismic Discontinuity Measures

The Local Structural Entropy

The Local Structural Entropy (LSE) is a measure of discontinuity, on a scale from zero to one. It indicates the degree of discontinuity within a given subvolume of the seismic data. By translating the 3-D seismic volume into a LSE volume, interpreters can often reveal subtle geological features, such as faults and channels, which are not readily apparent in the seismic data.

As a preprocessing stage for the computation of the LSE, each trace is modified by subtracting its mean value:

$$\hat{d}_{xyt} = d_{xyt} - E_t \{d_{xyt}\} = d_{xyt} - \frac{1}{N_t} \sum_{k=1}^{N_t} d_{xyk}, \quad (1)$$

where d_{xyt} and \hat{d}_{xyt} are respectively the original and modified t -th sample of the trace at position (x, y) , and N_t is the total number of samples in each trace.

Subsequently, a relatively small 3-D analysis cube is selected by the interpreter. The analysis cube moves throughout the 3-D modified seismic volume and outputs for each point a measure of LSE. The size and shape of the analysis cube defines the geometrical distribution of traces and samples to be used for the LSE computation. For the following discussion we assume that the analysis cube is a 3-D box enclosing $2L_1$ in-line traces, $2L_2$ cross-line traces and N samples. The analysis cube is split into four L_1 by L_2 by N quadrants, which are rearranged in a consistent fashion into column vectors $\{\mathbf{a}_i \mid i = 1, \dots, 4\}$. The correlation matrix of the analysis cube is formed from the correlations between the quadrants:

$$\mathbf{S} = \frac{1}{NL_1L_2} \begin{bmatrix} \mathbf{a}_1^T \mathbf{a}_1 & \cdots & \mathbf{a}_1^T \mathbf{a}_4 \\ \vdots & \ddots & \vdots \\ \mathbf{a}_4^T \mathbf{a}_1 & \cdots & \mathbf{a}_4^T \mathbf{a}_4 \end{bmatrix}. \quad (2)$$

This matrix contains on its diagonal the auto-correlations of individual quadrants, and on off-diagonals the cross-correlations between distinct quadrants \mathbf{a}_i and \mathbf{a}_j . It should be noted that the correlation matrix \mathbf{S} is symmetric, and that its six unique off-diagonal components correspond to two in-line, two cross-line, and two spatially-diagonal cross-correlations.

The LSE measure is associated with a distinguished point within the analysis cube, generically represented here by (x, y, t) . It is defined as the normalized trace of the corresponding correlation matrix:

$$\begin{aligned}\varepsilon(x, y, t) &= \frac{\text{tr } \mathbf{S}}{\|\mathbf{S}\|} - 1 = \frac{\sum_{i=1}^4 \mathbf{a}_i^T \mathbf{a}_i}{\sqrt{\sum_{i,j=1}^4 (\mathbf{a}_i^T \mathbf{a}_j)^2}} - 1 \\ &= \frac{\sum_{i=1}^4 \mathbf{a}_i^T \mathbf{a}_i}{\sqrt{\sum_{i=1}^4 \left[(\mathbf{a}_i^T \mathbf{a}_i)^2 + 2 \sum_{j=i+1}^4 (\mathbf{a}_i^T \mathbf{a}_j)^2 \right]}} - 1\end{aligned}\tag{3}$$

where $\|\cdot\|$ is the Hilbert-Schmidt norm (known also as the Frobenius or Euclidian norm) (Golub and Van Loan, 1996). If all the quadrants are perfectly correlated (minimum discontinuity), the elements of the correlation matrix are identical, so $\text{tr } \mathbf{S} = \|\mathbf{S}\|$ and $\varepsilon = 0$. If there is no correlation at all among the quadrants (maximum discontinuity), $\text{tr } \mathbf{S} \leq 2 \|\mathbf{S}\|$ and $\varepsilon \leq 1$. The structural entropy, in this respect, is a cost function that measures the amount of disorder (uncertainty) within an analysis cube. Notice that the LSE measure is assigned to a point which is not the center of the analysis cube. However, it is possible to space out the $(L_1 \text{ by } L_2 \text{ by } N)$ quadrants one trace apart on each side. In that case, the analysis cube encloses an odd number of traces on each side ($2L_1 + 1$ in-line traces and $2L_2 + 1$ cross-line traces), making it possible to associate the LSE measure with its center.

Normalized trace of the covariance matrix

Instead of subtracting the mean value from each trace and working with the correlation matrices, one can define discontinuity measures based on covariance matrices. In this case, the analysis cube moves throughout the 3-D *original* seismic volume. For each analysis cube, the covariances of the corresponding quadrants are computed and arranged into a matrix $\mathbf{\Sigma}$, whose normalized trace defines a discontinuity measure:

$$\varepsilon_1(x, y, t) = \frac{\text{tr } \mathbf{\Sigma}}{\|\mathbf{\Sigma}\|} - 1 = \frac{\sum_{i=1}^4 \sigma_{ii}^2}{\sqrt{\sum_{i=1}^4 \left[\sigma_{ii}^2 + 2 \sum_{j=i+1}^4 \sigma_{ij}^2 \right]}} - 1 \quad (4)$$

where σ_{ij}^2 are the elements of the covariance matrix. This measure can also be written as

$$\varepsilon_1(x, y, t) = \frac{\sum_{i=1}^4 \lambda_i}{\sqrt{\sum_{i=1}^4 \lambda_i^2}} - 1 \quad (5)$$

where $\{\lambda_i \mid i = 1, \dots, 4\}$ are the eigenvalues of $\mathbf{\Sigma}$ ¹.

It is easy to verify that ε_1 is also bounded between zero and one. If all the quadrants are perfectly correlated (minimum discontinuity), the components of the covariance matrix are identical. Accordingly, the rank of $\mathbf{\Sigma}$ is equal to one ($\mathbf{\Sigma}$ has a single nonzero eigenvalue λ_1) and $\varepsilon_1 = 0$. If there is no correlation at all among the quadrants (maximum discontinuity), then the maximum value of ε_1 occurs when all the eigenvalues of $\mathbf{\Sigma}$ are equal and, hence, $\varepsilon_1 \leq 1$.

¹In fact, the normalized trace of the correlation matrix \mathbf{S} (Eq. (3)) can also be written in terms of the eigenvalues of \mathbf{S} , since the trace of a matrix is equal to the sum of its eigenvalues, and the Hilbert-Schmidt norm of a matrix \mathbf{A} is equal to the trace of $\mathbf{A}^T \mathbf{A}$.

Generalized trace of the covariance matrix

The relation between ε_1 and the eigenvalues of the covariance matrix was obtained using the fact that the trace of the covariance matrix is equal to the sum of its eigenvalues, and the Hilbert-Schmidt norm of the covariance matrix is equal to the sum of the eigenvalues squared (Golub and Van Loan, 1996). Generally, we can define a discontinuity measure that is proportional to the ratio between ℓ_1 and ℓ_p ($p > 1$) norms of the vector of eigenvalues by

$$\varepsilon_{1,p}(x, y, t) = \alpha \left[\frac{\|\lambda\|_1}{\|\lambda\|_p} - 1 \right] = \alpha \left[\frac{\sum_{i=1}^4 \lambda_i}{\left(\sum_{i=1}^4 \lambda_i^p \right)^{\frac{1}{p}}} - 1 \right] = \alpha \left[\frac{2^{\frac{2}{p}-1} \text{tr } \Sigma}{[\text{tr } (\Sigma^p)]^{\frac{1}{p}}} - 1 \right], \quad (6)$$

where the constant $\alpha = (4^{1-\frac{1}{p}} - 1)^{-1}$ is a normalization factor, restricting the maximum value of $\varepsilon_{1,p}$ to one. In the special case where $p = 2$, $\varepsilon_{1,2} \equiv \varepsilon_1$, since $\|\Sigma\| = \|\lambda\|_2$.

Normalized scatter of the correlation matrix

If one is working with matrices of correlation coefficients, the energy of the off-diagonal components, suitably normalized, may be used for defining a measure of discontinuity. Specifically,

$$\varepsilon_2(x, y, t) = 1 - \sqrt{\frac{\|\mathbf{R}\|^2 - 4}{12}} = 1 - \sqrt{\frac{\sum_{i,j=1}^4 \rho_{ij}^2 - 4}{12}} \quad (7)$$

where \mathbf{R} is the matrix of correlation coefficients, whose elements are related to those of the covariance matrix by

$$\rho_{ij} = \frac{\sigma_{ij}}{\sqrt{\sigma_{ii}\sigma_{jj}}}, \quad i, j = 1, \dots, 4. \quad (8)$$

Again, the range of the discontinuity measure is between zero and one. If all the quadrants are perfectly correlated (minimum discontinuity), the components of \mathbf{R} are all ones, so $\|\mathbf{R}\|^2 = 16$

and $\varepsilon_2 = 0$. If there is no correlation at all among the quadrants (maximum discontinuity), the off-diagonal components of \mathbf{R} are all zero and $\varepsilon_2 = 1$.

Normalized scatter of the covariance matrix

A similar discontinuity measure, defined using the covariance matrix, is given by

$$\varepsilon_3(x, y, t) = 1 - \frac{\|\Sigma\|^2 - \sum_{i=1}^4 \sigma_{ii}^2}{\sum_{i=1}^4 \sum_{j \neq i}^4 \sigma_{ii} \sigma_{jj}} = 1 - \frac{\sum_{i=1}^3 \sum_{j=i+1}^4 \sigma_{ij}^2}{\sum_{i=1}^3 \sum_{j=i+1}^4 \sigma_{ii} \sigma_{jj}}. \quad (9)$$

In this case, the discontinuity is determined by the relative energy of the off-diagonal components (normalized scatter) of the covariance matrix. As before, we have $0 \leq \varepsilon_3 \leq 1$ and higher ε_3 values imply greater discontinuity.

Ratio between the second and first eigenvalues

As mentioned above, the eigenvalues of the covariance matrix are closely related to the degree of discontinuity within a prescribed analysis cube. Small amounts of discontinuity yield one large nonzero eigenvalue λ_1 , with the other eigenvalues being negligible. Higher degrees of discontinuity are observed when λ_2 , λ_3 and λ_4 become more significant. In particular, the ratio between the second and first eigenvalues can be used as a discontinuity measure:

$$\varepsilon_4(x, y, t) = \frac{\lambda_2}{\lambda_1}. \quad (10)$$

In general, the ratio of an eigenvalue to the summation of all eigenvalues expresses the percentage of the mean-square error introduced by eliminating the corresponding eigenvector (Rao 1968). In our case, when the quadrants of a given analysis cube are perfectly correlated, they can be represented

by a single eigenvector. Hence, the ratio between the second and first eigenvalues indicates a degree of inconsistency with a model of perfectly correlated quadrants ($0 \leq \varepsilon_4 \leq 1$ with higher ε_4 values implying greater discontinuity).

Normalized dominant eigenvalue

Another version of such a discontinuity measure could use the mean-square error introduced by eliminating all eigenvectors but the first. In this case, the discontinuity measure is proportional to the ratio between the summation of all eigenvalues besides λ_1 and the summation of all eigenvalues:

$$\varepsilon_5(x, y, t) = \frac{4}{3} \frac{\sum_{i=2}^4 \lambda_i}{tr \mathbf{\Sigma}} = \frac{4}{3} \left(1 - \frac{\lambda_1}{tr \mathbf{\Sigma}} \right) \quad (11)$$

where we have again normalized to keep the measure between 0 and 1.

It is worth mentioning that the above definitions are just examples of discontinuity measures, derived using the relations among quadrants of the analysis cubes. Other definitions can be obtained either by combining the above measures or using higher-order statistics, as will be shown in subsequent publications. The data examples that were tested showed slightly better results using ε_4 . However, the computational efficiency in estimating ε (Eq. (3)) made it the best candidate for quantifying seismic discontinuities.

Examples

In this section we use synthetic, as well as real, data examples to demonstrate the usefulness of the proposed discontinuity measures.

Synthetic data

A synthetic data was constructed, simulating a 3-D migrated seismic volume with two apparent faults. The data consist of 128 in-line traces and 128 cross-line traces, each containing 128 samples. A vertical cross-section through the synthetic seismic data is shown in Fig. 1a. A horizontal slice is shown in Fig. 2a. The corresponding slices through the LSE volumes, obtained with three different sizes of analysis cubes, are displayed in Figs. 1b-d and 2b-d. We used analysis cubes of sizes $[2 \ 2 \ 7]$, $[4 \ 4 \ 15]$ and $[6 \ 6 \ 31]$, where three numbers between the square brackets designate, respectively, the number of in-line traces, cross-line traces and number of time samples. The LSE values are mapped to shades of gray, where darker shades indicate greater discontinuity. Clearly, a smaller analysis cube yields a sharper image of the seismic discontinuity. Furthermore, regions of large structural dips give artifacts, when the analysis cube is too large.

To evaluate the performance of the LSE measure under noise conditions, we created a noisy version of the synthetic data, by adding a white Gaussian noise to the data values and a uniform noise to the phase of the seismic layers with a signal-to-noise ratio (SNR) of 5.6 dB. Specifically, the noisy data is given by

$$\tilde{d}_{xyt} = A_{xyt} \sin(\varphi_{xyt} + u_{xyt}) + n_{xyt} \quad (12)$$

where $d_{xyt} = A_{xyt} \sin(\varphi_{xyt})$ designates the clean simulated data, u_{xyt} is white uniform noise, and n_{xyt} is white Gaussian noise. The SNR is defined as the ratio between the variance of the original data and the mean square error, expressed in decibels as

$$SNR = 10 \log_{10} \frac{Var(d_{xyt})}{E \left[\left(d_{xyt} - \tilde{d}_{xyt} \right)^2 \right]}. \quad (13)$$

A vertical cross-section and horizontal slice through the noisy synthetic data are shown in Figs. 3a and 4a. The corresponding cross-sections and slices through the LSE volumes are presented in Figs. 3b-d and 4b-d. Compared to the original LSE volumes (Figs. 1 and 2), the LSE measure

evaluated for the noisy data is characterized by a higher SNR when a larger analysis cube is used. In this example, the SNR increases from -5.8 dB to 9.7 dB, by expanding the analysis cube from $[2 \ 2 \ 7]$ to $[6 \ 6 \ 31]$. However, the sensitivity to noise decreases at the price of generally reduced lateral resolution.

Real data

The real data example (courtesy of GeoEnergy) is from the Gulf of Mexico. The data is decimated in both time and space. The time interval is 8 ms , in-line trace spacing is 25 m , and cross-line trace spacing is 50 m . A small subvolume with an in-line distance of 5.025 km and a cross-line distance of 10.05 km (201×201 traces) is used for demonstration. Each trace is 1.808 s in duration (226 samples). Figs. 5a and 6a show, respectively, a horizontal slice at $t = 480 \text{ ms}$ and a vertical cross-section at $x = 2.5 \text{ km}$ through the seismic data. The corresponding cross-sections and slices through the LSE volumes, obtained with three different sizes of analysis cubes, are displayed in Figs. 5b-d and 6b-d. The size of the analysis cube is determined by the type of geological feature that is of interest to the interpreter. Structural features such as faults, having a longer vertical duration, are analyzed with a larger cube (lower resolution). Stratigraphic features such as channels, characterized by shorter vertical duration, are better resolved with smaller cubes (higher lateral resolution).

In addition to the LSE measure, we proposed six other local discontinuity measures, namely the normalized trace of the covariance matrix (ε_1), the generalized trace of the covariance matrix ($\varepsilon_{1,p}$), the normalized scatter of the correlation matrix (ε_2), the normalized scatter of the covariance matrix (ε_3), the ratio between the second and first eigenvalues (ε_4), and the normalized dominant eigenvalue (ε_5). These measures are closely related to the LSE measure, but entail a higher computational complexity. In Fig. 7 we compare these six alternative measures for the horizontal slice at $t = 480 \text{ ms}$, using an analysis cube of size $[6 \ 6 \ 31]$. The results are practically similar, but it was found

that ε_4 generally produces enhanced images with improved contrast between faults and background (*cf.* Fig. 7e). This may be attributed to the fact that principal eigenvalues are closely related to the local seismic structure, while smaller eigenvalues contribute noise to the measure.

Multiscale LSE Volumes

LSE volumes generated by smaller sizes of analysis cubes entail a lower computational complexity and provide a sharper image of seismic discontinuities. However, the sensitivity to noise and smaller-scale discontinuities, which are generally not of interest to an interpreter, increases as the size of the analysis cube is getting smaller. Hence, by combining LSE volumes using various sizes of analysis cubes, higher lateral resolutions can be obtained while restricting the detection of features to larger-scale discontinuities, such as fault surfaces.

Figs. 8 and 9 illustrate combinations of LSE volumes, using analysis cubes of $[2\ 2\ 7]$, $[4\ 4\ 15]$ and $[6\ 6\ 31]$ samples. Specifically, the multiscale LSE volumes are obtained by arithmetic mean of the LSE values (Figs. 8a and 9a), geometric mean (Figs. 8b and 9b), maximum LSE where its value is larger than a certain threshold (highly discontinuous regions) and minimum LSE elsewhere (Figs. 8c and 9c). The multiscale LSE volumes emphasize points, which are likely to be corresponding to fault surfaces. Such points are characterized by a high degree of discontinuity in all relevant scales.

Relation to Other Work

The local discontinuity measures proposed in this paper are closely related to the eigenstructure-based coherence computations (Gersztenkorn 1999). Gersztenkorn and Marfurt (1999) have shown that an eigendecomposition of the data covariance matrix (Gersztenkorn and Marfurt 1996a, 1996b; Kirilin 1992) provides a more robust measure of coherence, compared to cross correlation (Bahorich

and Farmer 1995, 1996) and semblance (Marfurt *et al.* 1998; Neidell and Taner, 1971) based computations. The eigenstructure-based coherence algorithm constructs for each point a J by J covariance matrix, where its (i, j) th component is a cross-covariance of the i th and j th traces within the analysis cube. Then, a coherence estimate is given by the ratio between the dominant eigenvalue and the trace of the covariance matrix. Fig. 10 shows horizontal slices at $t = 480ms$ and vertical cross-sections at $x = 2.5 km$ through the eigenstructure-based coherence volumes, obtained with analysis cubes of sizes $[4\ 4\ 15]$ and $[6\ 6\ 31]$ samples. For a comparison between the eigenstructure-based coherence algorithm and our LSE algorithm, let $[2L_1\ 2L_2\ N]$ denote the size of the analysis cube (*i.e.*, the analysis cube contains $2L_1$ in-line and $2L_2$ cross-line traces, each of N samples). The main differences between their algorithm and ours are as follows:

- Their algorithm computes cross-covariances of *traces*. Our method is based on cross-correlations of *subvolumes* (quadrants of the analysis cube).
- The size of the eigenstructure-based covariance matrix is $4L_1L_2 \times 4L_1L_2$, while the size of the LSE-based correlation matrix is only 4×4 .
- Their algorithm requires computations of dominant eigenvalues of large covariance matrices. Our algorithm avoids that.
- In terms of computational complexity, their algorithm requires $8(L_1L_2)^2N + 2L_1L_2(N + 2)$ multiplications and $8(L_1L_2)^2(N - 1) + 10L_1L_2(N - 1) + 4L_1L_2$ additions for the construction of a covariance matrix. Our method uses only $10L_1L_2N$ multiplications and $10(L_1L_2N - 1)$ additions for the construction of a 4×4 correlation matrix. For example, if the size of the analysis cube is $[6\ 6\ 21]$, then a computation of an eigenstructure-based covariance matrix needs 14,022 multiplications and 14,796 additions, whereas that of an LSE-based correlation matrix requires only 1,890 multiplications and 1,880 additions. We note that their computational complexity is even higher, compared to our algorithm, since their method needs also the first dominant

eigenvalues of the respective covariance matrices. Furthermore, as the analysis cube moves throughout the seismic data volume, the number of computations required for updating the LSE-based correlation matrix is significantly lower than that associated with the eigenstructure-based covariance matrix.

Conclusion

We have introduced an analysis method for the estimation of seismic local structural entropy, which is both robust to noise and computationally efficient. This method avoids the computation of large covariance matrices and eigenvalues, associated with the eigenstructure-based coherency estimates. Efficient discontinuity measures were proposed based on the relations between quadrants of the analysis cube. In particular, the Local Structural Entropy measure was found advantageous over the alternative measures, in terms of computational cost. Whereas the discontinuity measure, based on the ratio between the second and first eigenvalues, is advantageous in producing enhanced images with improved contrast between faults and background. By combining LSE volumes using various sizes of analysis cubes, we obtained a higher lateral resolution while suppressing smaller-scale discontinuities, which are generally not of interest to an interpreter. The robustness of the proposed method was demonstrated using synthetic and real data examples.

Acknowledgements

The authors would like to thank Dr. Anthony Vassiliou of GeoEnergy and Dr. Fred Warner of Yale University for valuable discussions and helpful suggestions.

References

- Bahorich, M. S., and Farmer, S. L., 1995, 3-D seismic discontinuity for faults and stratigraphic features: The Leading Edge, **14**, 1053–1058.
- Bahorich, M. S., and Farmer, S. L., 1996, Methods of seismic signal processing and exploration: US Patent 5 563 949.
- Gersztenkorn, A., 1999, Method and apparatus for seismic signal processing and exploration: US Patent 5 892 732.
- Gersztenkorn, A., and Marfurt, K. J., 1996a, Coherence computations with eigenstructure: 58th Conf. and Tech. Exhibition, Eur. Assn. Geosci. Eng., Extended Abstracts, X031.
- Gersztenkorn, A., and Marfurt, K. J., 1996b, Eigenstructure based coherence computations: 66th Ann. Internat. Mtg., Soc. Expl. Geophys., Extended Abstracts, 328–331.
- Gersztenkorn, A., and Marfurt, K. J., 1999, Eigenstructure-based coherence computations as an aid to 3-D structural and stratigraphic mapping: Geophysics, **64**, 1468–1479.
- Kirlin, R. L., 1992, The relationship between semblance and eigenstructure velocity estimators: Geophysics, **57**, 1027–1033.
- Marfurt, K. J., Kirlin, R. L., Farmer, S. L., and Bahorich, M. S., 1998, 3-D seismic attributes using a semblance-based coherency algorithm: Geophysics, **63**, 1150–1165.
- Marfurt, K. J., Sudhaker, V., Gersztenkorn, A., Crawford, K. D., and Nissen, S. E., 1999, Coherency calculations in the presence of structural dip: Geophysics, **64**, 104–111.
- Neidell, N. S., and Taner, M. T., 1971, Semblance and other coherency measures for multichannel data: Geophysics, **36**, 482–497.
- Rao, C. R., *Linear Statistical Inference and Its Applications*, Wiley, New York (1968).

Golub, G. H., and Van Loan, C. F., *Matrix Computations*, 3rd ed., Johns Hopkins University Press, Baltimore (1996).

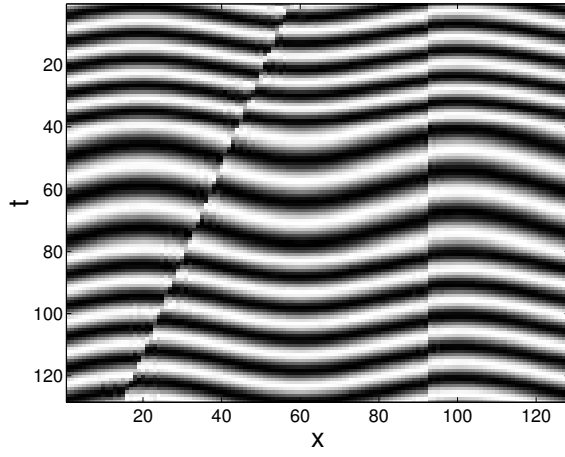
Figure Captions

- Fig. 1: Vertical cross-sections through (a) synthetic seismic data, and through the corresponding LSE volumes using analysis cubes of sizes (b) $[2 \ 2 \ 7]$, (c) $[4 \ 4 \ 15]$ and (d) $[6 \ 6 \ 31]$.
- Fig. 2: Horizontal slices through (a) synthetic seismic data, and through the corresponding LSE volumes using analysis cubes of sizes (b) $[2 \ 2 \ 7]$, (c) $[4 \ 4 \ 15]$ and (d) $[6 \ 6 \ 31]$.
- Fig. 3: Vertical cross-sections through (a) noisy synthetic seismic data (SNR=5.6 dB), and through the corresponding LSE volumes using analysis cubes of sizes (b) $[2 \ 2 \ 7]$ (SNR=-5.8 dB), (c) $[4 \ 4 \ 15]$ (SNR=4.0 dB) and (d) $[6 \ 6 \ 31]$ (SNR=9.7 dB).
- Fig. 4: Horizontal slices through (a) noisy synthetic seismic data (SNR=5.6 dB), and through the corresponding LSE volumes using analysis cubes of sizes (b) $[2 \ 2 \ 7]$ (SNR=-5.8 dB), (c) $[4 \ 4 \ 15]$ (SNR=4.0 dB) and (d) $[6 \ 6 \ 31]$ (SNR=9.7 dB).
- Fig. 5: Horizontal slices at $t = 480 \text{ ms}$ through (a) seismic data, and through the corresponding LSE volumes using analysis cubes of sizes (b) $[2 \ 2 \ 7]$, (c) $[4 \ 4 \ 15]$ and (d) $[6 \ 6 \ 31]$.
- Fig. 6: Vertical cross-sections at $x = 2.5 \text{ km}$ through (a) seismic data, and through the corresponding LSE volumes using analysis cubes of sizes (b) $[2 \ 2 \ 7]$, (c) $[4 \ 4 \ 15]$ and (d) $[6 \ 6 \ 31]$.
- Fig. 7: Horizontal slices at $t = 480 \text{ ms}$ through entropy volumes produced using six alternative entropy measures and an analysis cube of $[6 \ 6 \ 31]$ samples: (a) Normalized trace of the covariance matrix (ε_1). (b) Generalized trace of the covariance matrix ($\varepsilon_{1,8}$). (c) Normalized scatter of the correlation matrix (ε_2). (d) Normalized scatter of the covariance matrix (ε_3). (e) Ratio between the second and first eigenvalues (ε_4). (f) Normalized dominant eigenvalue (ε_5).
- Fig. 8: Combining LSE volumes using analysis cubes of $[2 \ 2 \ 7]$, $[4 \ 4 \ 15]$ and $[6 \ 6 \ 31]$ samples. Horizontal slices at $t = 480 \text{ ms}$ through: (a) Arithmetic mean of the LSE values. (b) Ge-

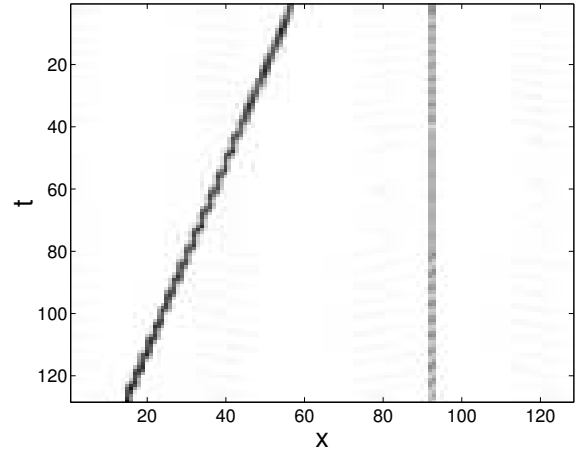
ometric mean of the LSE values. (c) Maximum LSE in highly discontinuous regions and minimum LSE elsewhere. (d) Maximum LSE in regions where both its value and its spatial average are higher than a certain threshold, and zero elsewhere.

Fig. 9: Combining LSE volumes using analysis cubes of $[2\ 2\ 7]$, $[4\ 4\ 15]$ and $[6\ 6\ 31]$ samples. Vertical cross-sections at $x = 2.5\ km$ through: (a) Arithmetic mean of the LSE values. (b) Geometric mean of the LSE values. (c) Maximum LSE in highly discontinuous regions and minimum LSE elsewhere. (d) Maximum LSE in regions where both its value and its spatial average are higher than a certain threshold, and zero elsewhere.

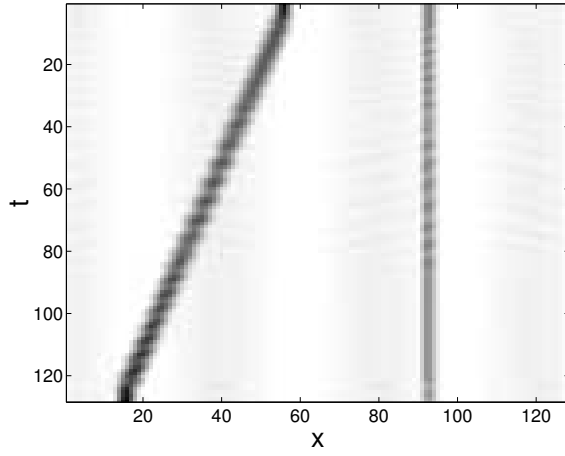
Fig. 10: Eigenstructure-based coherence images: Horizontal slices at $t = 480\ ms$ using analysis cubes of (a) $[4\ 4\ 15]$ samples, and (b) $[6\ 6\ 31]$ samples. Vertical cross-sections at $x = 2.5\ km$ using analysis cubes of (c) $[4\ 4\ 15]$ samples, and (d) $[6\ 6\ 31]$ samples.



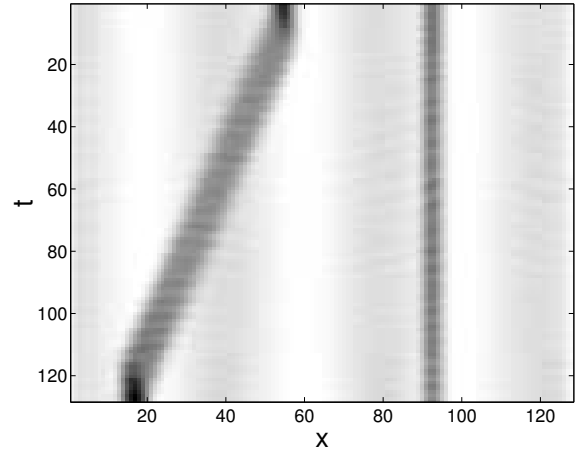
(a)



(b)

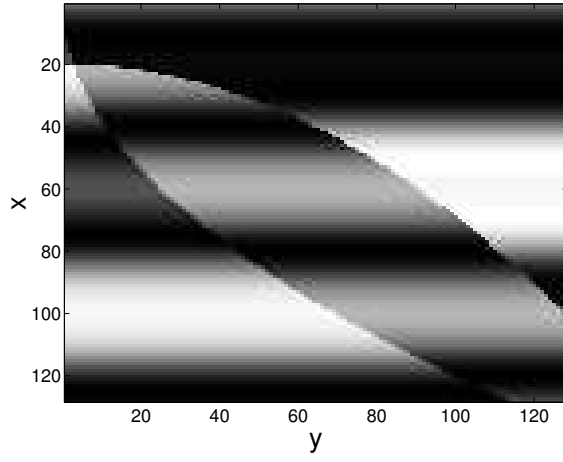


(c)

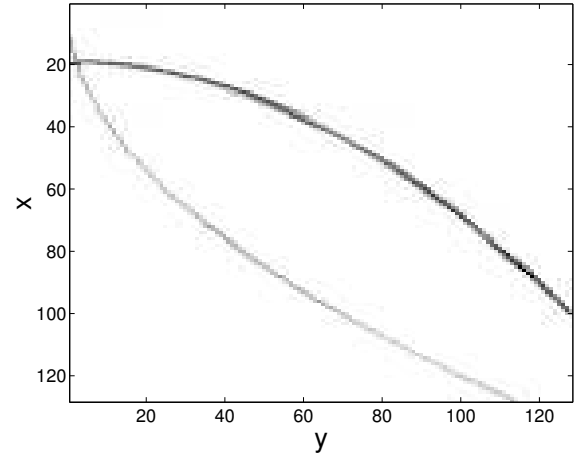


(d)

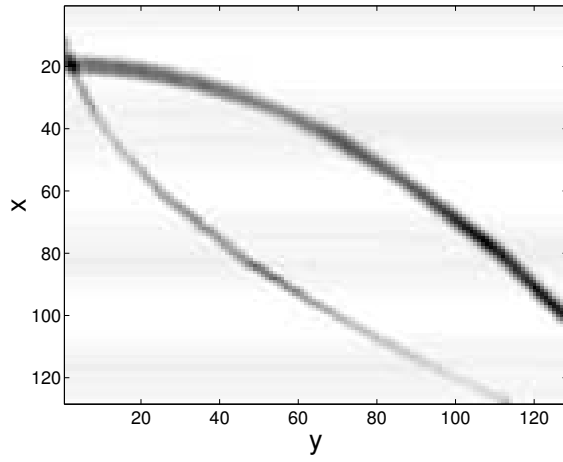
Figure 1: Vertical cross-sections through (a) synthetic seismic data, and through the corresponding LSE volumes using analysis cubes of sizes (b) $[2\ 2\ 7]$, (c) $[4\ 4\ 15]$ and (d) $[6\ 6\ 31]$.



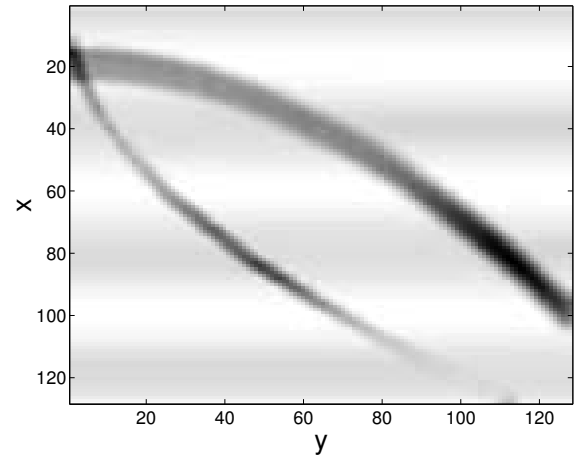
(a)



(b)

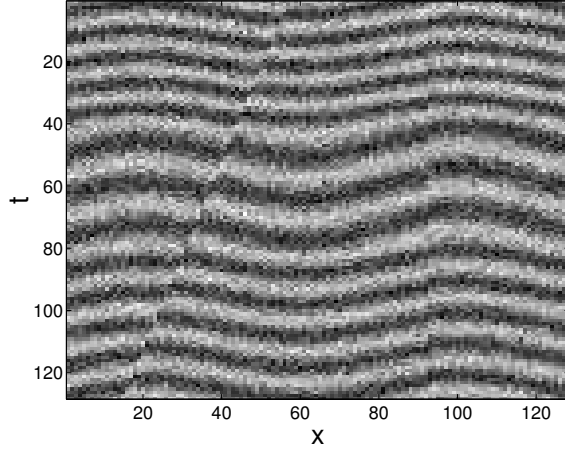


(c)

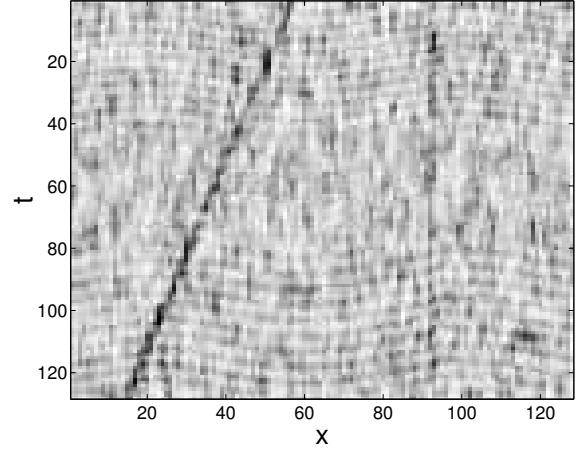


(d)

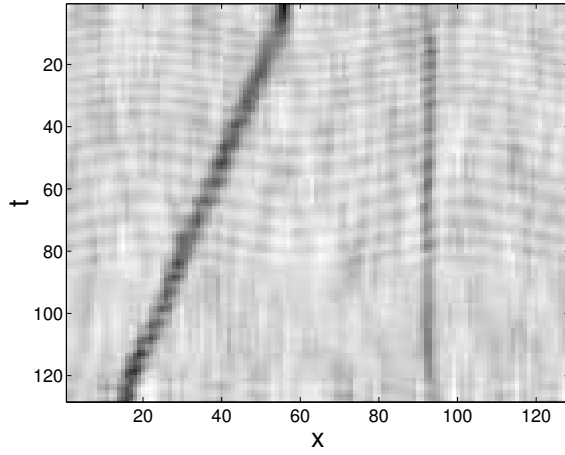
Figure 2: Horizontal slices through (a) synthetic seismic data, and through the corresponding LSE volumes using analysis cubes of sizes (b) $[2 \ 2 \ 7]$, (c) $[4 \ 4 \ 15]$ and (d) $[6 \ 6 \ 31]$.



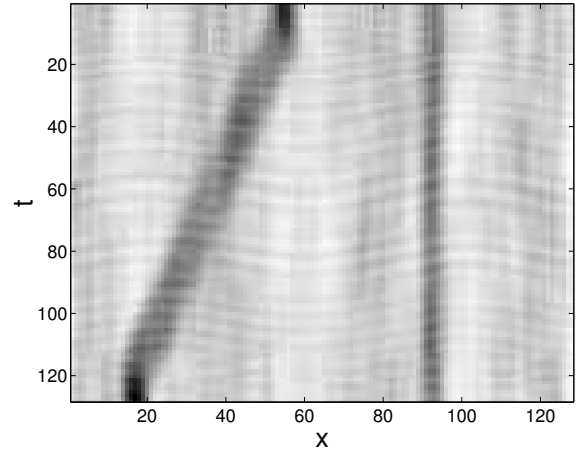
(a)



(b)

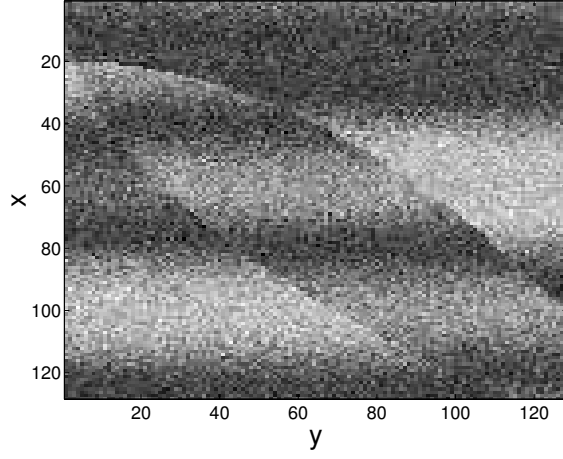


(c)

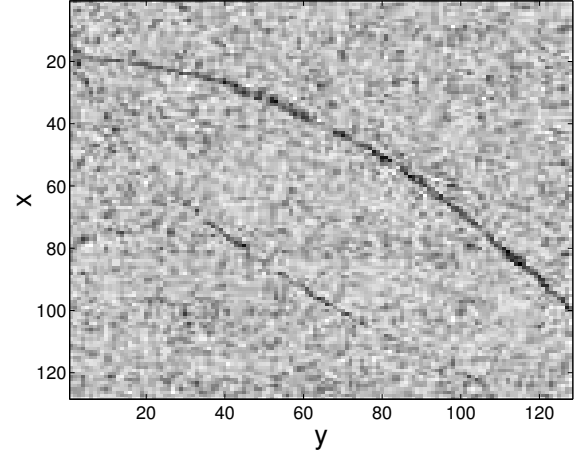


(d)

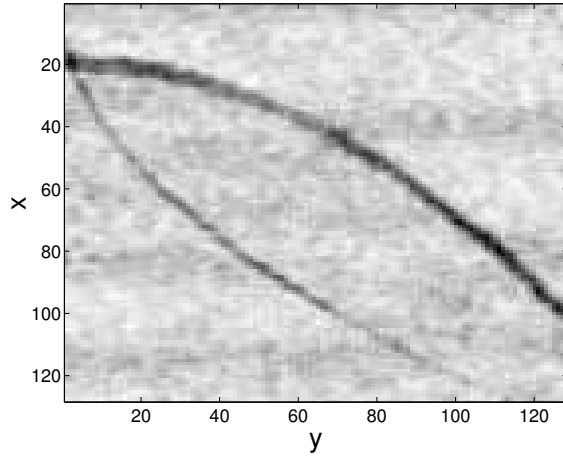
Figure 3: Vertical cross-sections through (a) noisy synthetic seismic data (SNR=5.6 dB), and through the corresponding LSE volumes using analysis cubes of sizes (b) $[2 \ 2 \ 7]$ (SNR=-5.8 dB), (c) $[4 \ 4 \ 15]$ (SNR=4.0 dB) and (d) $[6 \ 6 \ 31]$ (SNR=9.7 dB).



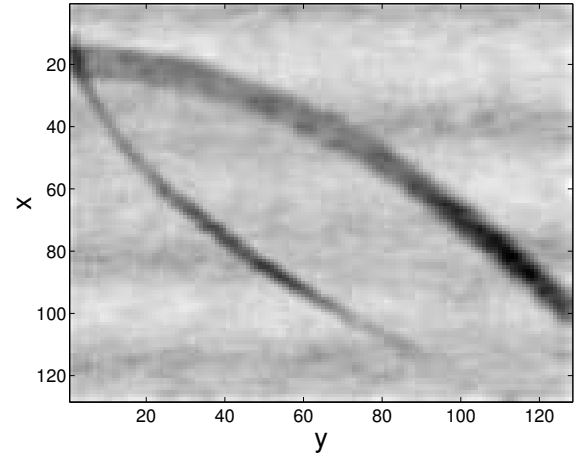
(a)



(b)

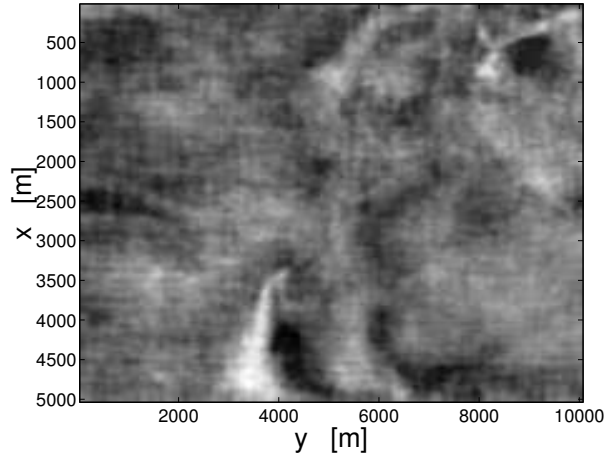


(c)

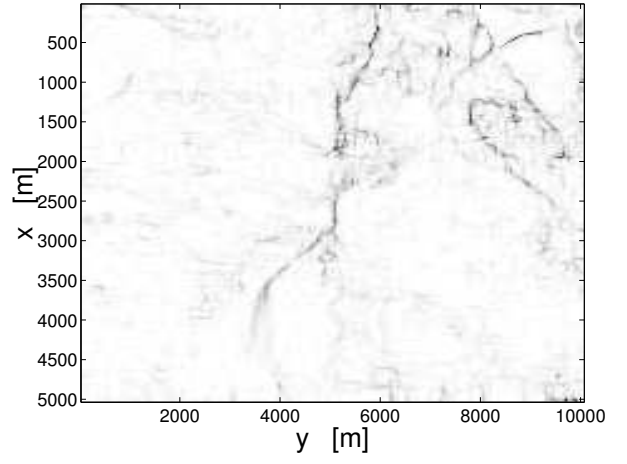


(d)

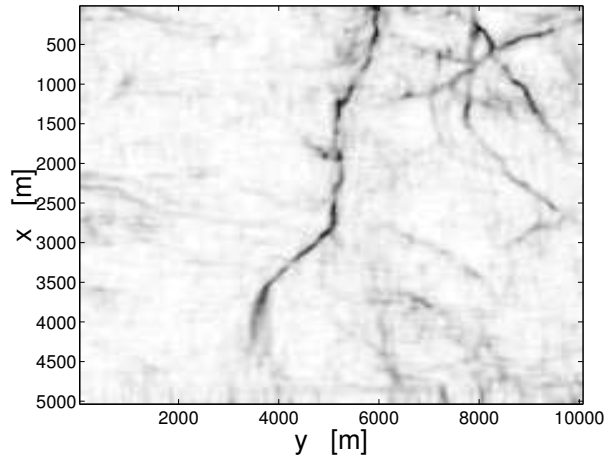
Figure 4: Horizontal slices through (a) noisy synthetic seismic data (SNR=5.6 dB), and through the corresponding LSE volumes using analysis cubes of sizes (b) $[2 \ 2 \ 7]$ (SNR=-5.8 dB), (c) $[4 \ 4 \ 15]$ (SNR=4.0 dB) and (d) $[6 \ 6 \ 31]$ (SNR=9.7 dB).



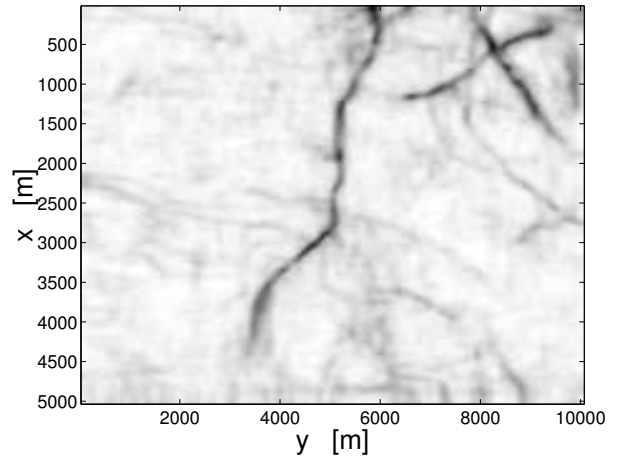
(a)



(b)

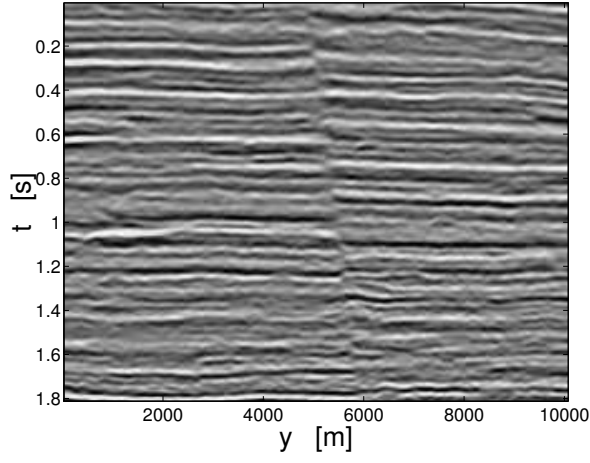


(c)

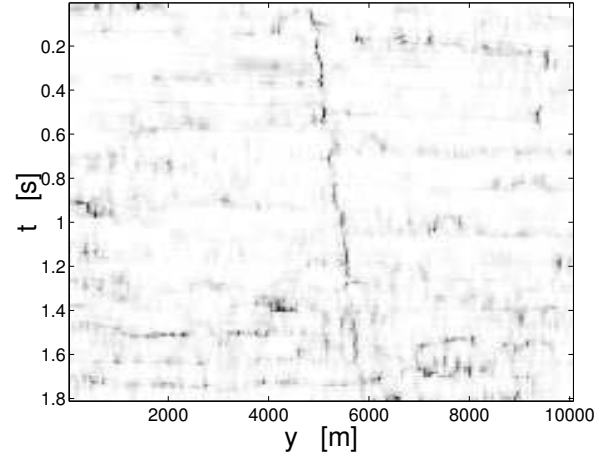


(d)

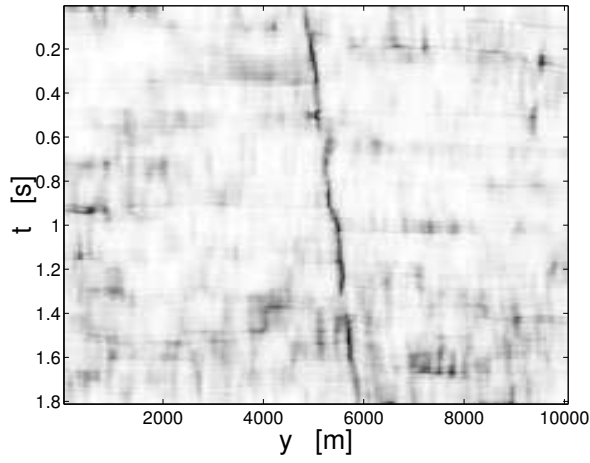
Figure 5: Horizontal slices at $t = 480 \text{ ms}$ through (a) seismic data, and through the corresponding LSE volumes using analysis cubes of sizes (b) $[2 \ 2 \ 7]$, (c) $[4 \ 4 \ 15]$ and (d) $[6 \ 6 \ 31]$.



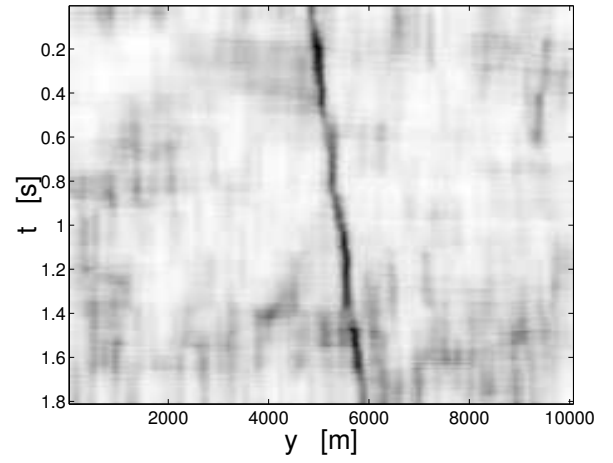
(a)



(b)

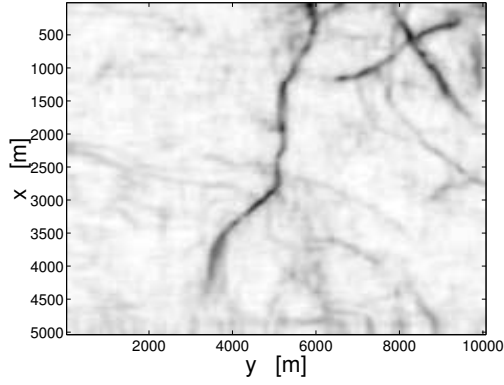


(c)

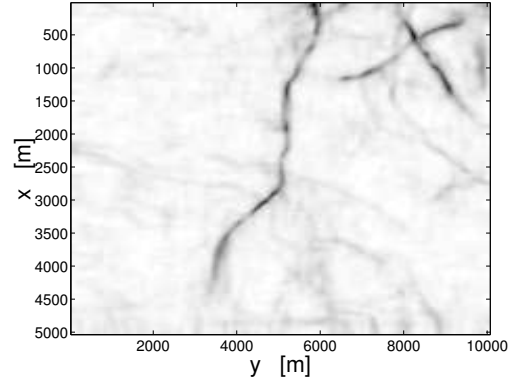


(d)

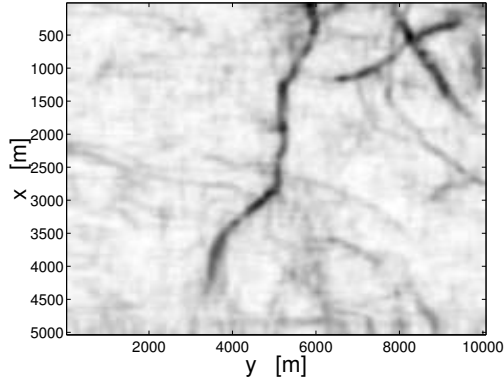
Figure 6: Vertical cross-sections at $x = 2.5 \text{ km}$ through (a) seismic data, and through the corresponding LSE volumes using analysis cubes of sizes (b) $[2 \ 2 \ 7]$, (c) $[4 \ 4 \ 15]$ and (d) $[6 \ 6 \ 31]$.



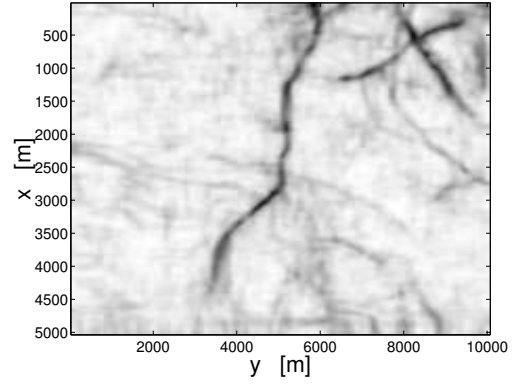
(a)



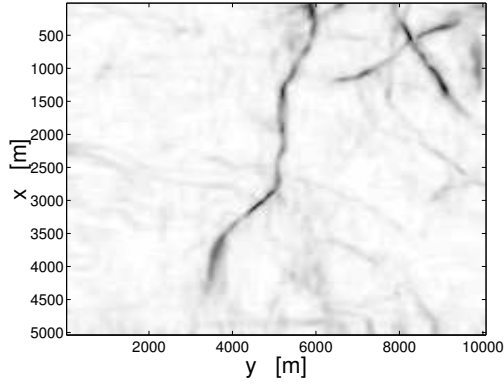
(b)



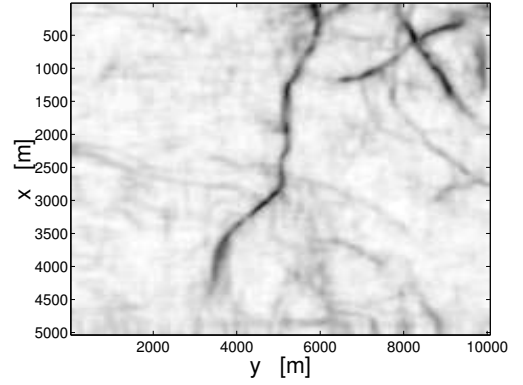
(c)



(d)



(e)



(f)

Figure 7: Horizontal slices at $t = 480ms$ through entropy volumes produced using six alternative entropy measures and an analysis cube of $[6\ 6\ 31]$ samples: (a) Normalized trace of the covariance matrix (ε_1). (b) Generalized trace of the covariance matrix ($\varepsilon_{1,8}$). (c) Normalized scatter of the correlation matrix (ε_2). (d) Normalized scatter of the covariance matrix (ε_3). (e) Ratio between the second and first eigenvalues (ε_4). (f) Normalized dominant eigenvalue (ε_5).

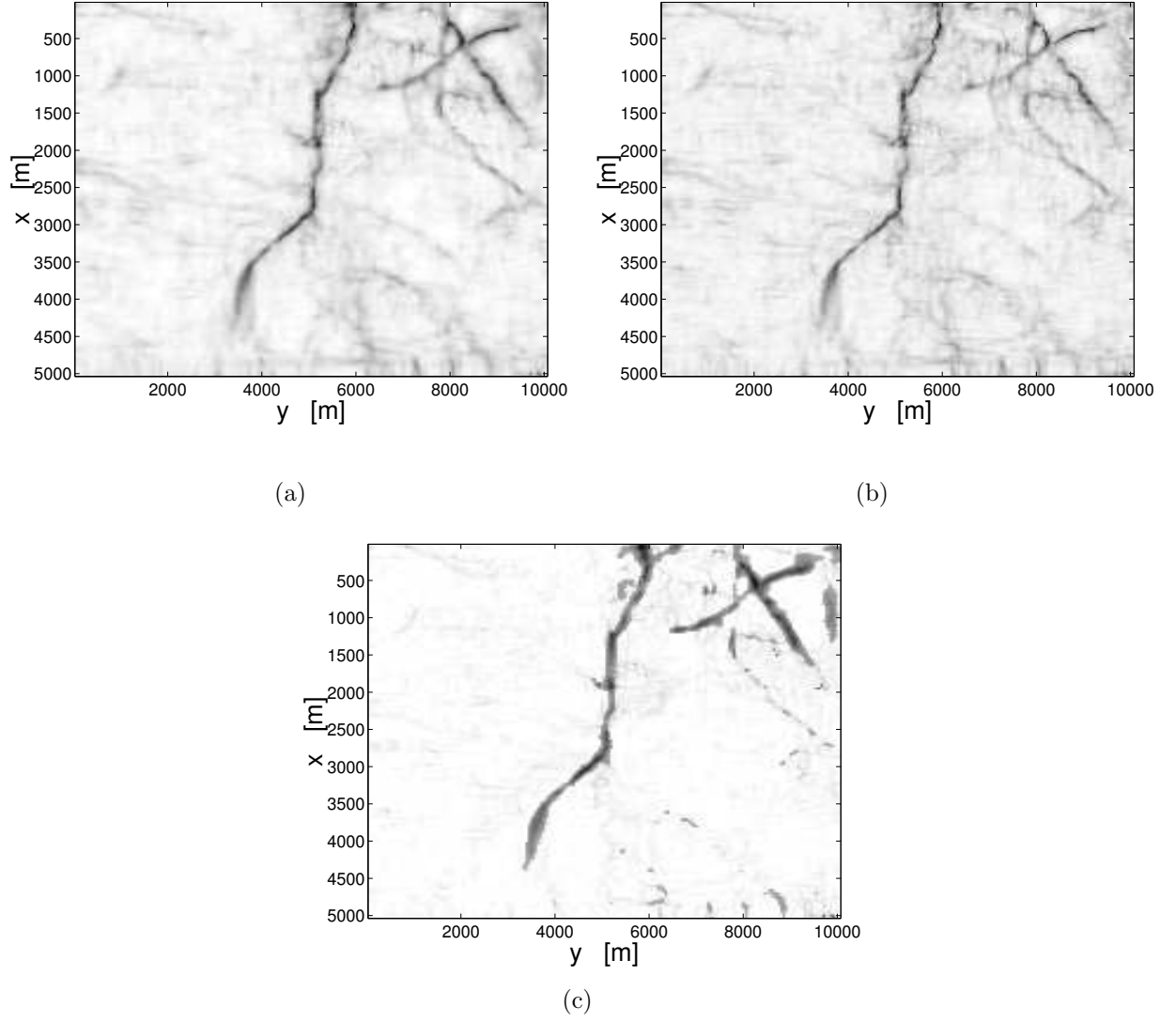
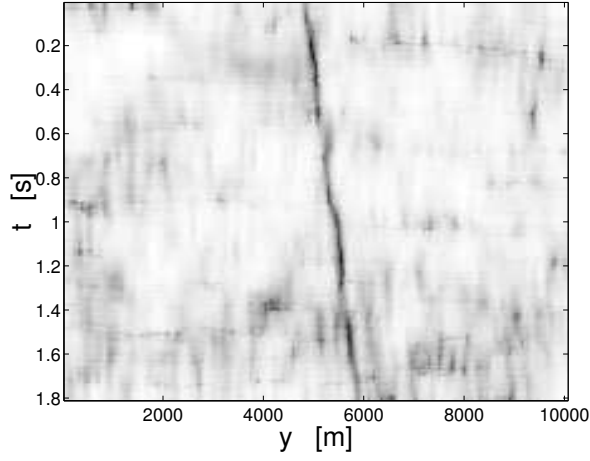
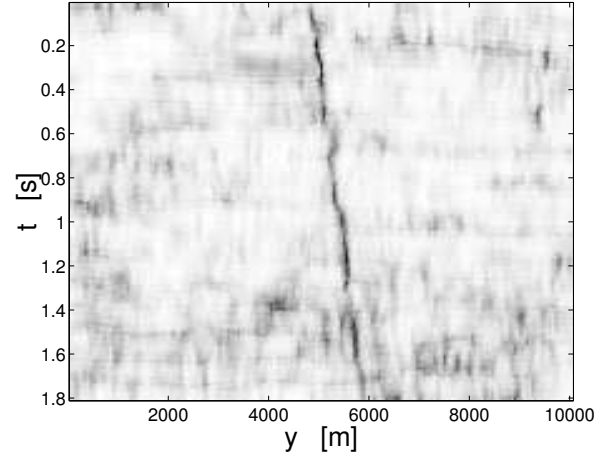


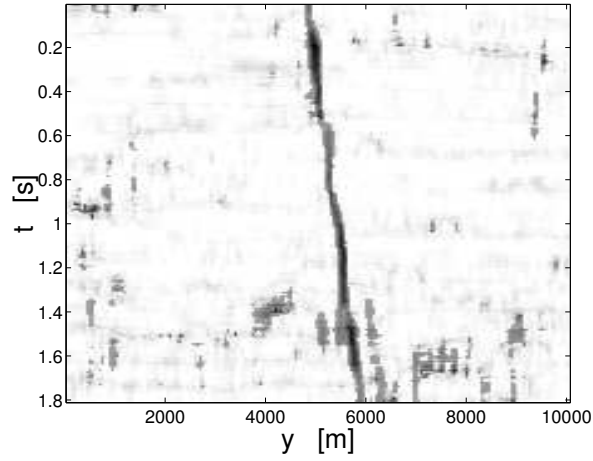
Figure 8: Combining LSE volumes using analysis cubes of $[2 \ 2 \ 7]$, $[4 \ 4 \ 15]$ and $[6 \ 6 \ 31]$ samples. Horizontal slices at $t = 480 \text{ ms}$ through: (a) Arithmetic mean of the LSE values. (b) Geometric mean of the LSE values. (c) Maximum LSE in highly discontinuous regions and minimum LSE elsewhere.



(a)

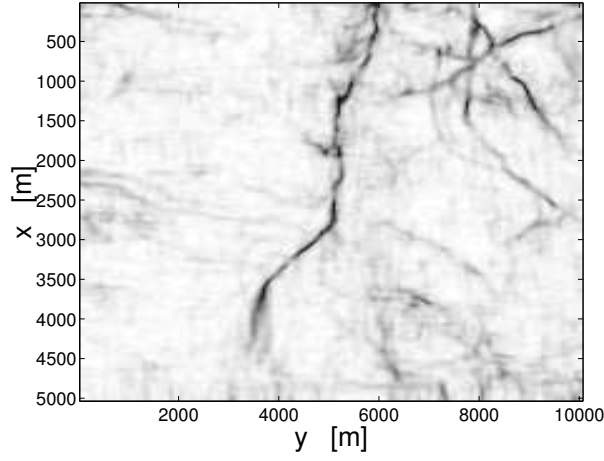


(b)

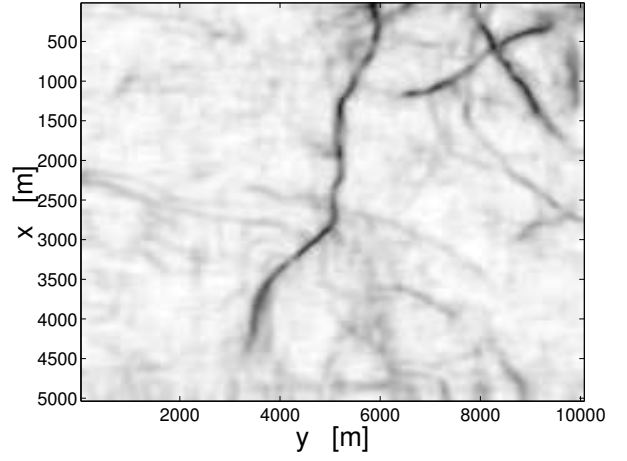


(c)

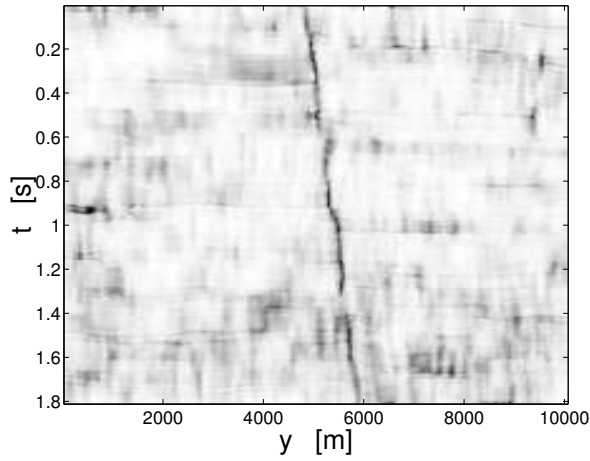
Figure 9: Combining LSE volumes using analysis cubes of $[2\ 2\ 7]$, $[4\ 4\ 15]$ and $[6\ 6\ 31]$ samples. Vertical cross-sections at $x = 2.5\ km$ through: (a) Arithmetic mean of the LSE values. (b) Geometric mean of the LSE values. (c) Maximum LSE in highly discontinuous regions and minimum LSE elsewhere.



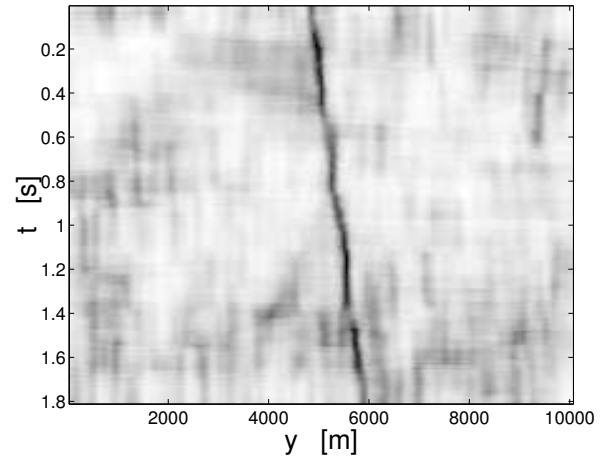
(a)



(b)



(c)



(d)

Figure 10: Eigenstructure-based coherence images: Horizontal slices at $t = 480ms$ using analysis cubes of (a) $[4\ 4\ 15]$ samples, and (b) $[6\ 6\ 31]$ samples. Vertical cross-sections at $x = 2.5\ km$ using analysis cubes of (c) $[4\ 4\ 15]$ samples, and (d) $[6\ 6\ 31]$ samples.